Optimizing Second-Order Nonlinear Materials for Bright Quantum State Generation: A Genetic Algorithm Approach

Colin Dietrich [1,*], Joseph Lamarre[1,2], Stéphane Virally[1,†] and Nicolas Godbout[1,2]

[1] *Polytechnique Montréal, 2500 chemin de Polytechnique, Montréal, QC H3T 1JK, Canada*
[2] *Castor Optics Inc, 361 Boulevard Montpellier, Saint-Laurent, QC H4N 2G6, Canada*

[*] *colin.dietrich@polymtl.ca*, [†] *stephane.virally@polymtl.ca*

Abstract: An innovative genetic algorithm for the inverse design of second-order nonlinear materials is presented. It aims at optimizing the generation of bright entangled states. The approach offers potential breakthroughs in advanced quantum state engineering.

1. introduction

Optical imaging and metrology have recently seen remarkable advancements, particularly with the use of non-classical light sources that enhance resolution and reduce noise [2–4]. Yet, the emission of individual photon streams from these sources poses challenges, especially in noisy environments [5]. One widely publicized achievement with much brighter non-classical sources was in gravitational wave detection via the use of a bright squeezed state in the LIGO interferometer [1].

To facilitate their adoption in broader applications, it is thus necessary to develop non-classical light sources with significantly higher photon rates. These have significant potential in techniques like Fourier Transform Infrared Spectroscopy (FTIR) [6], Electro-optic Sampling (EOS) [23], and Optical Coherence Tomography [7].

The cornerstone of bright quantum sources lies in second-order nonlinear materials that enable phenomena such as Spontaneous Parametric Down-Conversion (SPDC) and Second Harmonic Generation (SHG) [15, 16]. Modulating the nonlinear susceptibility in these materials can significantly influence the efficiency and spectral characteristics of the resulting optical processes.

The importance of such modulation has seen a surge in the development of inverse design techniques aiming at optimizing crystal structures for diverse applications [12–14]. While various methods, from machine learning [11] to algorithms like simulated annealing [10] and Monte Carlo [9], have emerged, challenges persist in achieving an ideal entangled photon source characterized by high photon rates, spectral purity, and broadband performance.

This paper presents a genetic algorithm approach to address these challenges. Drawing inspiration from natural evolution, this algorithm focuses on crafting optimal crystal designs. Its efficiency, especially in fields where the search space is vast and the landscape of potential solutions has numerous local optima, has been validated in previous studies [17–19].

2. Methodology

2.1. *Problem formulation*

As depicted in Figure 1(a), nonlinear crystals are modeled as segmented into N domains, each of a specific width, Λ. This width corresponds to the coherence length of the nonlinear process under consideration, defined as $\Lambda = \pi/\Delta k$ [15, 16]. Each domain has an orientation, d, which can take values of either $+1$ or -1. Collectively, these domains define the nonlinear profile of the crystal, forming the set of unknown parameters, Θ, in the inverse problem:

$$\Theta = \{d_1, d_2, ..., d_{N-1}, d_N\} \tag{1}$$

The observable, $\mathbf{O}$, which represents the output state of the crystal, can be equated to the spectra of the signal and idler fields in the SPDC process taking place inside the crystal. These observables help gauge how closely the unknown parameters align with the target observable, $\mathbf{O}_\mathrm{t}$.

The dynamics of the system are encapsulated in the forward simulation, $\Gamma(\cdot)$. This simulation takes the unknown parameters as input and yields an observable. The inverse design problem thus becomes finding the unknown parameters, Θ, for a given set of observables $\mathbf{O}_t$ [11]

$$\Theta = \Gamma^{-1}(\mathbf{O}_\mathrm{t}), \tag{2}$$

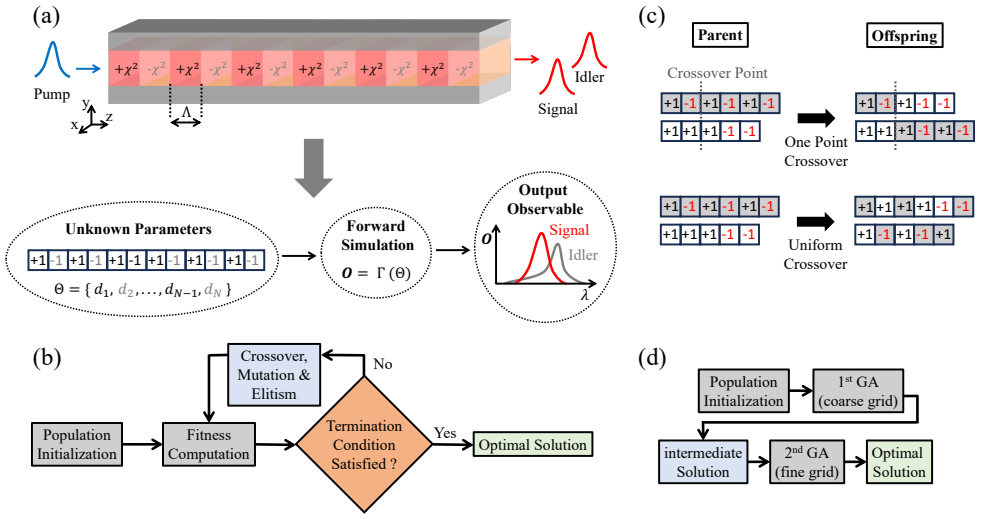

Fig. 1. (a) Representation of the inverse problem. (b) Diagram of the genetic algorithm. (c) One-point and uniform crossover diagram. (d) Diagram of the enhanced genetic algorithm.

where Γ^{-1} represents the inverse problem.

To evaluate the alignment between a given observable, $\mathbf{O}$, and the desired observable, $\mathbf{O}_t$, a mean-square error fitness function is employed:

$$f = \sum_{k=1}^{M} \frac{(O_k - O_{tk})^2}{M}. \tag{3}$$

2.2. *System dynamics*

The focus is on the dynamics of second-order nonlinear processes within thin-film nonlinear crystals. Given the thin nature of these films, an assumption of a uniform transverse field distribution is made, which simplifies calculations. This assumption is well-justified, especially in thin-film waveguides where core dimensions are significantly smaller than the photon wavelength, resulting in an almost constant transverse field distribution [20]. The nonlinear coupled modes equations for these processes are derived from Heisenberg's equations of motion [21,22]:

$$\begin{aligned}
\frac{\partial \hat{A}_\mathrm{i}(z,\omega_\mathrm{i})}{\partial z} &= \frac{\omega_\mathrm{i}^2}{c^2 k_\mathrm{i}(\omega_\mathrm{i})}\chi_2(z)\int \mathrm{d}\omega_\mathrm{s}\, e^{-i\Delta k(\omega_\mathrm{i},\omega_\mathrm{s})} A_\mathrm{p}(z,\omega_i+\omega_s)\hat{A}_\mathrm{s}^\dagger(z,\omega_\mathrm{s});\\
\frac{\partial \hat{A}_\mathrm{s}(z,\omega_\mathrm{s})}{\partial z} &= \frac{\omega_\mathrm{s}^2}{c^2 k_\mathrm{s}(\omega_\mathrm{s})}\chi_2(z)\int \mathrm{d}\omega_\mathrm{i}\, e^{-i\Delta k(\omega_\mathrm{i},\omega_\mathrm{s})} A_\mathrm{p}(z,\omega_\mathrm{i}+\omega_\mathrm{s})\hat{A}_\mathrm{i}^\dagger(z,\omega_\mathrm{i});\\
\frac{\partial A_\mathrm{p}(z,\omega_\mathrm{p})}{\partial z} &= \frac{\omega_\mathrm{p}^2}{c^2 k_\mathrm{p}(\omega_\mathrm{p})}\chi_2(z)\int \mathrm{d}\omega_i\, e^{i\Delta k(\omega_\mathrm{i},\omega_\mathrm{p}-\omega_\mathrm{i})} \hat{A}_\mathrm{s}(z,\omega_\mathrm{p}-\omega_\mathrm{i})\hat{A}_\mathrm{i}(z,\omega_\mathrm{i}),
\end{aligned} \tag{4}$$

where the subscripts i, s, and p correspond to the idler, signal, and pump fields, respectively. For a field labeled by the subscript x, its angular frequency is denoted by ω_x, and its wavenumber is represented by k_x. χ_2 is the second-order nonlinear susceptibility, considered constant over the range of wavelengths. Δk is the phase mismatch between the interacting waves [15]. The envelope operator $\hat{A}_\mathrm{x}$ is derived from the electric field operator, as $\hat{E}(\mathbf{r},\omega) = e^{ik_z(\omega)z}A(\mathbf{r}_\perp,\omega)\hat{A}(z,\omega)$ where $A(\mathbf{r}_\perp,\omega)$ is the normalized transverse mode profile [11,25]. The system equations are numerically integrated using the fourth-order Runge-Kutta method, as detailed in Ref. [26]. The implementation uses JAX, a specialized just-in-time compiler designed for high-performance accelerator code generation, compatible with Python and Numpy-based frameworks [27].

2.3. *Genetic algorithm*

As illustrated in Figure 1(b), the genetic algorithm operates in four stages [17–19, 24]: **(1)** Initialization of a population where n crystal designs are randomly generated or according to a rule specified by the user. **(2)** Forward simulation to compute the output observable and the fitness function of each design. **(3)** A termination condition set by the user, such as reaching a maximum number of iterations or achieving a desired fitness threshold. **(4)** If the termination condition is not met, the algorithm employs genetic mechanisms like mutation, crossover, elitism, and

natural selection to produce offspring [24]. The fittest crystals are then selected from both the parent and offspring populations.

The crossover and mutation are presented in more detail in Figure 1(c). In genetic algorithms, one-point crossover selects a random point on parent chromosomes and swaps their segments, uniform crossover mixes genes from parents at each position based on random choice, and mutation introduces small random changes in offspring genes [24]. A key attribute of this algorithm is its adaptability in determining crystal length. During initialization, it randomly sets the domain count for each crystal, ensuring lengths vary within the problem's constraints. As the algorithm progresses, these lengths can adjust to achieve optimality.

3. Results and discussion

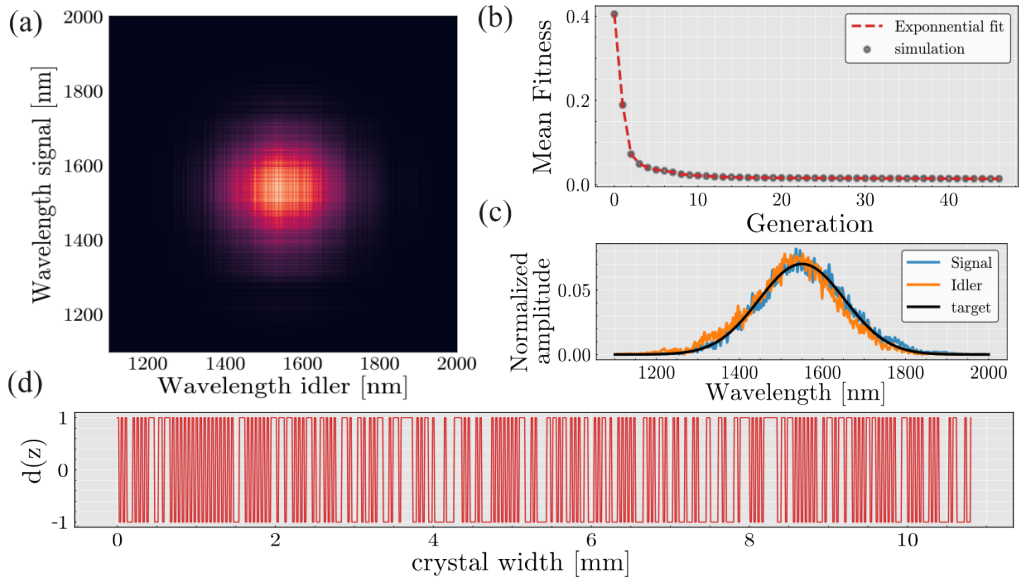

Fig. 2. (a) Joint Spectral amplitude of signal and idler fields for the best crystal of the first generation. (b) Evolution of the mean fitness as a function of the generation. (c) Spectrum of signal and idler fields for the best crystal of the last generation. (d) Poling function of the best crystal of the last generation.

Figure 2 presents the genetic algorithm results applied for a type-II SPDC process, utilizing a Gaussian pump pulse centered at 775 nm with a 60 nm bandwidth. The Potassium Titanyl Phosphate (KTP) crystal has a width ranging from 1 to 1.5 cm. The target function, a Gaussian centered at 1550 nm with a 60 nm bandwidth, is juxtaposed with the signal and idler spectra to achieve spectral purity and optimal biphoton entanglement. The genetic algorithm starts with 50 crystal configurations initialized as periodically-poled KTPs (PPKTPs) and is iterated over 50 generations. Figures 2(a) and 2(b) present respectively the symmetric Joint Spectral Amplitude and the signal and idler fields spectra for the optimal crystal of the last generation. Figure 2(b) illustrates a consistent improvement in mean fitness across generations. While the current solution approaches the desired outcome, shows symmetric spectral correlations, and validates the model, enhancements are under consideration. Increasing the population size could boost convergence and further improve the mean fitness, potentially yielding superior outcomes. Additionally, unlike other inverse design methods discussed earlier, the genetic algorithm can optimize parameters beyond just the poling profile, encompassing the selection among various crystal types and the polarization of the fields. To achieve this, greater computational power is required. Specifically, Figure 1(c) suggests optimizing the genetic algorithm by running it on a coarse grid, followed by a finer discretization to refine the results. Note that this model is also applicable to other second-order nonlinear phenomena such as SHG.

References

1. The LIGO Collaboration,"Enhanced sensitivity of the LIGO gravitational wave detector by using squeezed states of light", in *Nature Photonics* **7**, 613 (2013).
2. K.C. Tan and H. Jeong,"Nonclassical light and metrological power : An introductory review", in *AVS Quantum Science* **1**, 014701 (2019).
3. V. Giovannetti, S. Lloyd and L. Maccone,"Advances in quantum metrology", in *Nature Photonics* **5**, 222 (2011).

4. Moreau, PA., Toninelli, E., Gregory, T. et al. “Imaging with quantum states of light”, in *Nat Rev Phys* **1**, 367–380 (2019).
5. M.D. Eisaman, J. Fan, A. Migdall and S.V. Polyakov, “Single-photon sources and detectors”, in *Review of Scientific Instruments* **82**, 071101 (2011).
6. A. Dutta, “Spectroscopic methods for nanomaterials characterization”, chapter 4, “Fourier transform infrared spectroscopy”, in *Elsevier series on micro and nano technologies*, (2017).
7. N. Eladawi et al., “Diabetes and Fundus OCT”, chapter 7, “Optical coherence tomography : a review” in *Elsevier series on computer-assisted diagnosis*, (2020).
8. G.M. D’Ariano, M. De Laurentis, M.G.A. Paris, A. Porzio and S. Solimeno, “Quantum tomography as a tool for the characterization of optical devices”, in *Journal of Optics B : Quantum and Semiclassical Optics* **4**, S127 (2002).
9. Elier Ramos-Israde, Karina Garay-Palmett, and Roger S. Cudney, “Randomly aperiodically poled LiNbO3 crystal design by Monte Carlo–Metropolis with simulated annealing optimization for ultrabroadband photon pair generation”, in *Appl. Opt.* **60**, 10587-10593 (2021).
10. Graffitti, F. et al., “Pure Down-Conversion Photons through Sub-Coherence-Length Domain Engineering”, in *Quantum Science and Technology 2* **3**, 035001 (2017).
11. Eyal Rozenberg, Aviv Karnieli, Ofir Yesharim, Joshua Foley-Comer, Sivan Trajtenberg-Mills, Daniel Freedman, Alex M. Bronstein, and Ady Arie, “Inverse design of spontaneous parametric downconversion for generation of high-dimensional qudits”, in *Optica* **9**, 602-615 (2022).
12. Ma, W., Liu, Z., Kudyshev, Z.A. et al., “Deep learning for the design of photonic structures”, in *Nat. Photonics* **15**, 77–90 (2021).
13. Ren, S. et al., “Inverse deep learning methods and benchmarks for artificial electromagnetic material design”, in *Nanoscale 14* **10**, 3958–3969 (2022).
14. Peter R. Wiecha, Arnaud Arbouet, Christian Girard, and Otto L. Muskens, “Deep learning in nano-photonics: inverse design and beyond”, in *Photon. Res.* **9**, B182-B200 (2021).
15. Christ A. et al., “Experimental Methods in the Physical Sciences”, chapter 11, “Parametric Down-Conversion” in *Academic Press* **9**, 351–410 (2013).
16. Ali Anwar, Chithrabhanu Perumangatt, Fabian Steinlechner, Thomas Jennewein, Alexander Ling, “Entangled photon-pair sources based on three-wave mixing in bulk crystals”, in *Rev. Sci. Instrum.* **92**, 351–410 (2021).
17. Siyang Xiao et al., ”Inverse design of a near-infrared metalens with an extended depth of focus based on double-process genetic algorithm optimization.”, in *Optics Express* **31**, 484471 (2023).
18. Rithwik Tom et al., ”Inverse Design of Tetracene Polymorphs with Enhanced Singlet Fission Performance by Property-Based Genetic Algorithm Optimization”, in *Chemistry of Materials* **35**, 2c03444 (2023).
19. Z. He, K. Yuan, G. Xiong, and J. Wang, ”Inverse Design and Experimental Verification of Metamaterials for Thermal Illusion Using Genetic Algorithms”, in *Chinese Physics Letters* **35**, 104402 (2023).
20. Lihong Hong, Lingzhi Peng, Zhiyuan Li, ”Theoretical solution of second-harmonic generation in periodically poled lithium niobate and chirped periodically poled lithium niobate thin film via quasi-phase-matching”, in *Phys. Rev. A* **104**, 053503 (2021).
21. Mitchell M. W., ”Parametric Down-Conversion from a Wave-Equation Approach: Geometry and Absolute Brightness”, in *Phys. Rev. A* **79**, 043835 (2009).
22. Brambilla, E. et al, ”Simultaneous near-field and far-field spatial quantum correlations in the high-gain regime of parametric down-conversion”, in *Phys. Rev. A* **69**, 023802 (2004).
23. Virally, S., Cusson, P. and Seletskiy, D.V., ”Enhanced Electro-optic Sampling with Quantum Probes”, in *Physical Review Letters* **127**, 270504 (2004).
24. Katoch, S., Chauhan, S.S. and Kumar, V., ”A review on genetic algorithm: past, present, and future”, Chapter 3, ”Quantum-Mechanical Theory of the Nonlinear Optical Susceptibility”, Multimedia Tools and Applications”, in *Multimed Tools Appl* **80**, 8091–8126 (2021).
25. Boyd, R.W., ”Nonlinear Optics (Third Edition)”, Multimedia Tools and Applications”, in *R.W. Boyd (ed.)*, 135–206 (2008).
26. Zhang, Z., Chen, L. and Bao, X., ”A fourth-order Runge-Kutta in the interaction picture method for numerically solving the coupled nonlinear Schrödinger equation”, in *Optics Express*, **18** 8261–8276 (2010).
27. James Bradbury et al., ”JAX: composable transformations of Python+NumPy programs”, http://github.com/google/jax (2018).